Fibers and Polymers 2011, Vol.12, No.4, 438-443 DOI 10.1007/s12221-011-0438-0

Fabrication and Characterization of Nano Al_2O_3 Filled PVA:NH_4SCN Electrolyte Nanofibers by Electrospinning

Navin Chand, Neelesh Rai[1]*, T. S. Natarajan[2], and S. L. Agrawal[1]

Advanced Materials and Processes Research Institute (AMPRI) (Formerly RRL) (CSIR) Habibganj Naka, Bhopal, India
[1]*SSI Laboratory, Department of Physics, APS University, Rewa (M.P.), India*
[2]*Department of Physics, Indian Institute of Technology, Madras, India*

(Received August 22, 2010; Revised January 15, 2011; Accepted January 20, 2011)

Abstract: Present paper reports a method of preparing polymer composite electrolyte nanofiber mat using polyvinyl alcohol (PVA), ammonium thiocyanate (NH_4SCN) salt, and aluminium oxide (Al_2O_3) nano particles based on electrospinning technique. Two-stage process of preparation of nanofibers, namely, preparation of nano particles filled PVA electrolyte gel solution followed by its electrospinning has been used. The so obtained nanofibers have been characterized by XRD, DSC, SEM, and Conductivity measurements. XRD patterns affirm the formation of nanocomposite while SEM pictures reveal formation of fibers on a nano scale format (300-800 nm). Fibers of the electrolytes are seen to be thermally stable. Ionic conductivity of electrolyte fiber is seen to improve in the presence of nano filler at room temperature with a maximum at 5.31×10^{-3} Scm^{-1} for 4 wt% filler concentration, which is comparable to that for corresponding dried gel electrolyte films.

Keywords: Ionic conductivity, Electrolyte nanofibers, Nanocomposites, Electrospinning, Polyvinyl alcohol

Introduction

Over the years, polymer gel electrolytes have been given impetus in electrochemical devices due to certain distinct advantages over solid polymer electrolytes, particularly, ionic conductivity that approaches to that of liquid electrolytes [1-4]. However, these gel electrolytes possess soft morphology (on account of liquid trapped within the polymer matrix) which limits their use in polymer battery and fuel cell applications. Oozing of liquid at high temperature is one of the severest problems of gel electrolytes that can lead to internal short circuit. Recently, researchers have dispersed fillers in gel matrix to form polymer composite gel electrolytes to circumvent the problem of liquid oozing to a great extent [5,6]. However, such electrolytes show lack of good mechanical and electrochemical stability.

Various other techniques like phase inversion and emersion precipitation have been recently developed to synthesise highly conducting electrolyte membranes. In the phase inversion method [7,8], nanoporous membranes with high porosity, large surface area, and excellent mechanical property have been produced. Though, polymer electrolytes based on this method show good mechanical property, factors like electrochemical stability are adversely affected by the presence of residual solvent. Immersion precipitation method has also been tried to prepare microporous structured electrolytes [9]. Such electrolytes have been shown to possess fast ion mobility and high ionic conductivity besides maintaining mechanical integrity.

There is yet another approach to prepare high yield microporous polymer matrix by electrospinning of polymer solution [10,11]. In electrospinning technique, nanofibers can be deposited at a rate of several meters per second [12] with easy evaporation of solvent. Evaporation of solvent is related to phase separation in polymer gel and it influences the fiber diameter and surface morphology [13]. Such nanofibrous membranes have been shown to exhibit high porosity with pore size of a few tens of nanometer to a few micrometers, interconnected open pore structure and large surface area per unit mass. Besides, electrospun fibers have been shown to possess high mechanical and electrochemical stability thus making them important class of material for electrochemical and medical applications. Electrospun fibers have been examined for applications in drug delivery, nanosensors, photovoltaic devices, etc [14].

The favorable properties of electrospun fibers have been tested by few workers in development of electrolyte nanofibers mat for fuel cell and battery applications [15-17]. In all these reports, the electrospun nanofibers have been prepared directly from spinning the polymer solution. The ionic conductivities of such fibers in some cases seem to augment while in the other it detoriates [16,18]. Some of the popularly used polymers like Poly(ethylene oxide) (PEO), Poly(vinyl alcohol) (PVA), Poly(aniline) (PANI), Poly(vinyl pyrrolidone) (PVP), and Poly(vinylidene fluoride) (PVdF) have been used as the polymer matrix for development of nanofibers mat in recent past [15,16,19-23]. Because of solvent swollen ability, high solubility, good gelling property, and being a good stabilizer of noble metals, PVA has been popularly used in nanofiber production [24-26]. Further, literature survey shows that there is dearth of PVA based fibers for electrochemical device applications.

Thus in the present work, an attempt has been made to develop PVA based electrospun nanocomposite electrolyte

---

*Corresponding author: neeleshssi@gmail.com

mats for applicability in various ionic devices in general and smart windows and drug delivery system in particular. The fibers investigated here are expected to improve the morphology thus rendering higher ionic conduction with improved mechanical integrity which is important for efficient working of smart windows and drug delivery system. This preliminary investigation comprises of development of polyvinyl alcohol:ammonium thiocynate:aluminium oxide ($PVA:NH_4SCN:Al_2O_3$) nanocomposite electrolyte fibers followed by their structural, thermal, and electrical characterization.

Experimental

Materials and Preparation of Gel Solution

In the present investigation, PVA (average molecular weight 124,000-186,000, Aldrich make), ammonium thiocyanate (NH_4SCN), AR grade, and aprotic solvent dimethyl sulphoxide (DMSO) were used for synthesis of composite gels. Al_2O_3 used in the study was obtained from Alfa Aesar, CAS Number: 1344-28-1 possessing average particle size in between 40 and 50 nm. PVA was dispersed in 1 M salt solution of NH_4SCN in DMSO in different stoichiometric ratios to form pristine gel electrolyte (PVA: NH_4SCN system). Composite polymer gel electrolyte viscous solutions were prepared by adding Al_2O_3 nano particles in pristine gel electrolyte solution in different weight proportions followed by thorough mixing at slightly elevated temperature on a magnetic stirrer for four hours. These solutions were subsequently used to electrospin nanofibers of this electrolyte.

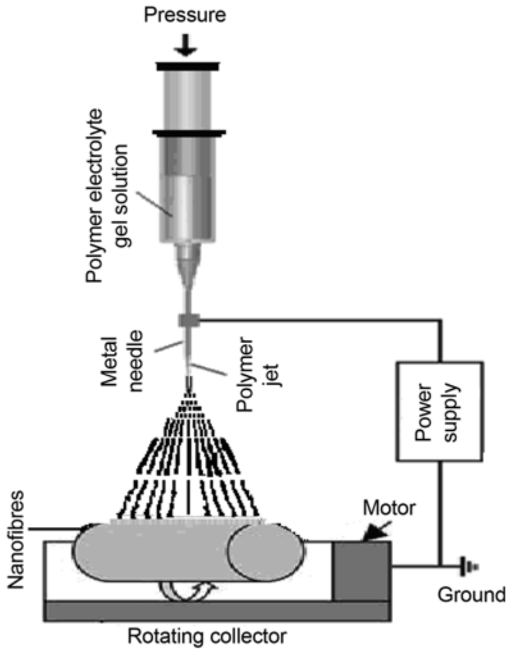

Figure 1. Schematic diagram of electrospinning setup for making nanofibers.

Preparation of Nanofibers

Nanofibers of $PVA:NH_4SCN:DMSO:Al_2O_3$ were prepared using electrostatic spinner coupled with a high voltage dc power supply. In the experiment, dc voltage was set at 22 kV while the distance between the spinneret and the fiber collector was mechanically adjusted at 14 cm to achieve good quality of fibers at room temperature (28 °C). In the first step of experiment, the gel solution of $PVA:NH_4SCN:DMSO:Al_2O_3$ was prepared by solution cast technique as described earlier. In step 2, this gel solution was filled in the syringe and a voltage of 22 kV was applied to the gel solution. A mat of fibers was formed over aluminium foil and collected for further characterization. A schematic representation of the electrospinning setup used in this study is shown in Figure 1.

Characterization of Nanofibers

Scanning Electron Microscopy (SEM)

The surface morphology of electrostatic spun fibers was observed using a JEOL scanning electron microscope (Model JSM-6390A). A very thin coating of gold was applied to the fibers in a sputtering unit before using the samples for examination of surface morphology. These pictures were also used to estimate the diameter of fibers.

Differential Scanning Calorimetry (DSC)

Thermal measurements were performed using a Mettler Toledo make Differential Scanning Calorimetry (model 822e). Thermal scan of fiber samples was carried out in open air environment at a heating rate of 10 °C/min. in the temperature range 40-280 °C.

XRD Measurements

X-ray diffraction (XRD) patterns of fibers were recorded on an X-ray Diffractometer (RIGAKU, JAPAN make, model MINIFLEX-II). The diffraction patterns were recorded at

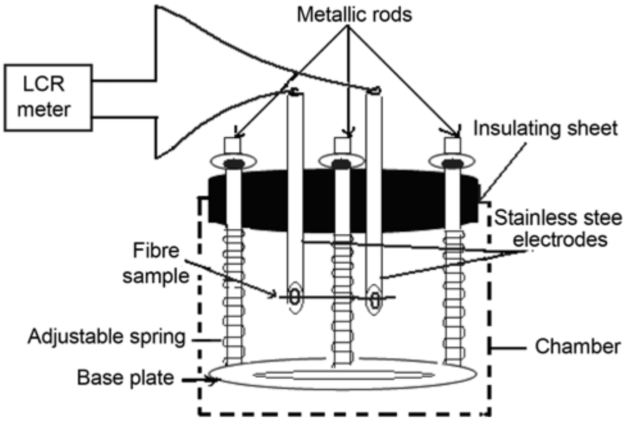

Figure 2. Schematic diagram of two probes for measuring resistivity of fibers.

room temperature (~25 °C) for the Bragg angle (2θ) varying from 2 to 90 °.

Conductivity Measurements

Complex-impedance spectra were recorded in the frequency range 40 Hz-100 KHz with help of a computer controlled LCR meter (Hioki Japan, make model 3520). The fiber samples were placed between two stainless steel needle electrodes. Schematic diagram of sample holder is shown in Figure 2.

Results and Discussion

Fabrication of Electrolyte Nanofibers and Morphological Studies

In the initial electrospinning process, droplets of electrolyte were observed to form on the collector. Generally this process can be associated to loss of polymeric chain entanglement as also reported earlier by Sanders *et al.* [27]. Fabrication of nano fibers in electrospinning process is known to depend upon several factors like concentration of solution, adjustment of spraying needle from collector, flow rate, applied voltage, etc [20,28,29]. To improve the quality of fibers one of the possible ways is to make the solution viscous by evaporating solvents and for this reason the gel solution was heated slightly on a magnetic stirrer to achieve viscous gel solution for electrospraying. This led to formation of nano fibers though with extremely low yield (Figure 3(a)). In the next step, salt solution (NH_4SCN) was added to form fibers of pristine electrolyte PVA:NH_4SCN. This effectively not only allowed to develop nano fibers of pristine electrolyte but also improved the yield of nano fibers (Figure 3(b)).

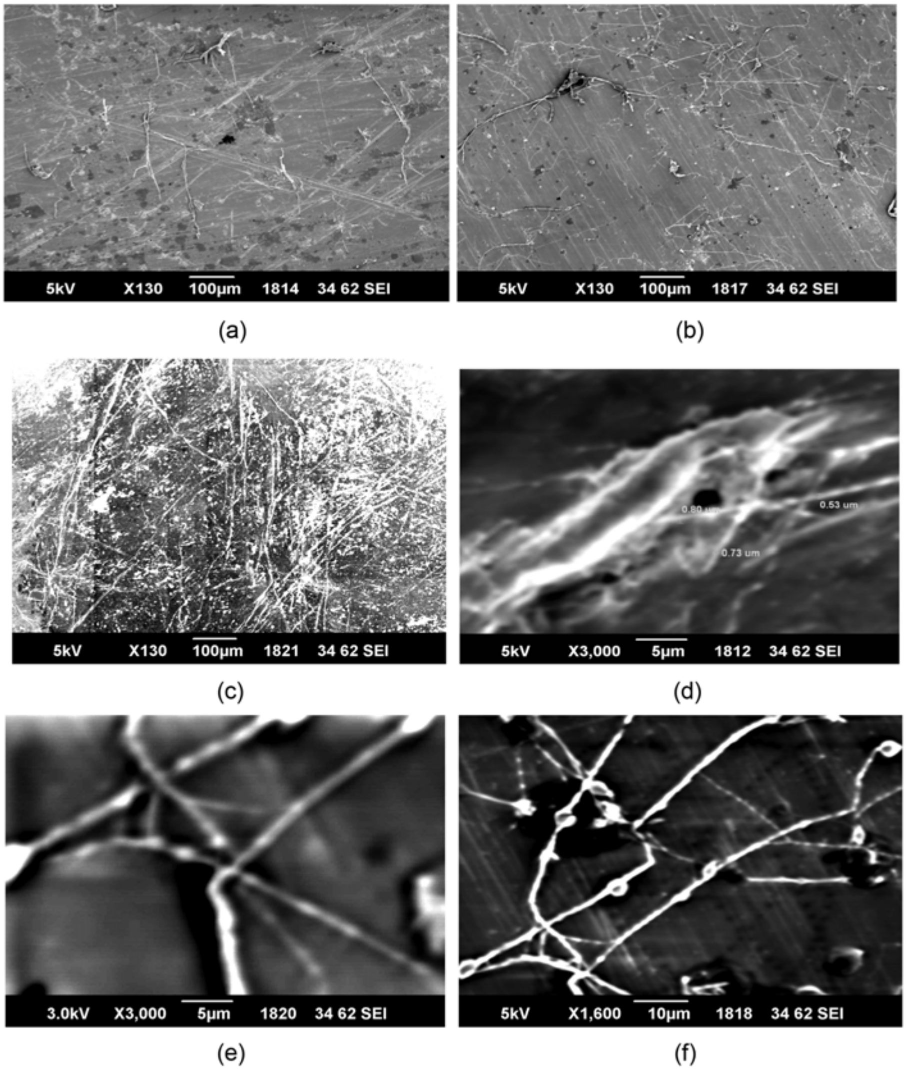

Figure 3. SEM Image of (a) PVA:DMSO nanofibers mat, (b) PVA:DMSO:NH_4SCN nanofibers mat, (c) PVA:DMSO:NH_4SCN+4 wt% Al_2O_3 nano filled nanofiber mat with low magnification, (d) PVA:DMSO:NH_4SCN+2 wt% Al_2O_3 nano filler filled nanofibers, (e) PVA:DMSO:NH_4SCN+4 wt% Al_2O_3 nano filler filled nanofibers, and (f) PVA:DMSO:NH_4SCN+6 wt% Al_2O_3 nano filler filled nanofibers.

Subsequently, Al_2O_3 was added in gel electrolyte solution to form nanofibers of polymer composite electrolyte. This led to further improvement in the yield of nanofibers (Figure 3(c)). In order to study the effect of nano aluminium oxide on the formation of fiber, Al_2O_3 content in polymer electrolyte solution was varied stoichiometrically from 0 to 6 wt%. It was observed that beyond 6 wt% nano Al_2O_3 filled PVA electrolyte became too viscous to be processed which resulted in unstable electrospraying. In all the electrospinning experiments, electric field was adjusted to obtain a perfectly stable electrospinning jet. These conditions were obtained for a flow rate of 0.4 m*l*/h. This optimum value of flow rate was selected after varying the flow rate between 0.1 to 0.6 m*l*/h and examining the yield and quality of nanofibers.

Figure 3(a)-(f) shows the surface morphology of PVA: DMSO, PVA:DMSO:NH_4SCN fibers, and polymer nanocomposite electrolyte fibers containing 2, 4, and 6 wt% of Al_2O_3 nanofiller. During SEM examination of PVA:DMSO fibers (Figure 3(a)), the nanofibers are seen to be randomly and sparsely distributed. Same morphology is observed for PVA: DMSO:NH_4SCN electrolyte fibers but with improvement in fiber length and yield (Figure 3(b)). Figure 3(c) shows the morphology of 4 wt% nano Al_2O_3 filled PVA electrolyte fibers on 100 μm scale. It is apparent from SEM picture that the yield of fibers increases on addition of filler though the length of fiber is distributed. Also beading effect is noticed in fiber mats as indicated by appearance of white protruded dots along the length of fibers at few places. To see the impact of Al_2O_3 concentration on morphology of fibers, SEM picture for different Al_2O_3 contents were recorded at higher magnification (Figure 3(d) to 3(f)). It is observed that on increasing the nano Al_2O_3 contents in the PVA electrolyte to form composite electrolyte, more uniform fibers were obtained. This might be due to interaction among components as witnessed in XRD study to be discussed later on. In this microstructure, Al_2O_3 grains are visible within the fibers dispersed homogeneously upon careful examination of SEM pictures. Such an arrangement is likely to promote conduction pathways for mobile ions viz. possibly protons. Measurement of diameter of these nanofibers ascertained their nanometric format with average diameter being 560 nm.

XRD Studies

The XRD patterns of nano Al_2O_3 filled and unfilled PVA electrolyte nanofibers along with pristine components are shown in Figure 4. These patterns show in general an increase in amorphousness of polymer fibers on addition of salt and Al_2O_3 nanofiller. The XRD pattern for PVA:DMSO nanofiber (Figure 4(c)) exhibits shifting of PVA related peak (around 20.1 °) towards lower 2θ value (19.02 °) on addition of salt NH_4SCN in PVA matrix (Figure 4(d)). Additionally, a shoulder peak at 2θ=15.4° appears in PVA-NH_4SCN nano fiber. Both peaks do not match to either salt or polymer and hence corroborates the formation of a new material viz. PVA-NH_4SCN complex. Further increase in d value for all the major peaks and shifting of peak towards lower 2θ value with broadening, indicates improvement in morphology of PVA-NH_4SCN complex upon electrospinning of fibers. Also, upon addition of Al_2O_3 nano filler (Figure 4(e)), the peaks seem to further broaden up besides emergence of a broad peak around 26.4°. This broad peak related to PVA-NH_4SCN-Al_2O_3 complex appears on account of interaction of electrolyte with Al_2O_3 leading to formation of nanocomposite fiber as this doesn't correspond to any of the pristine materials PVA, Al_2O_3, and NH_4SCN. Further no other peak related to Al_2O_3 could be tracked in the composite nanofibers to suggest the role of Al_2O_3 as of passive filler in composite fiber. On increasing Al_2O_3 content, the new peak is seen to shift to lower 2θ value with increasing broadness. This feature again ascertains improvement in system morphology with complete absorption of Al_2O_3 particles in PVA matrix electrolyte. From X-ray diffraction study, it is thus concluded that Al_2O_3 nanofillers upon dispersal drastically improves the amorphous behavior of electrolyte.

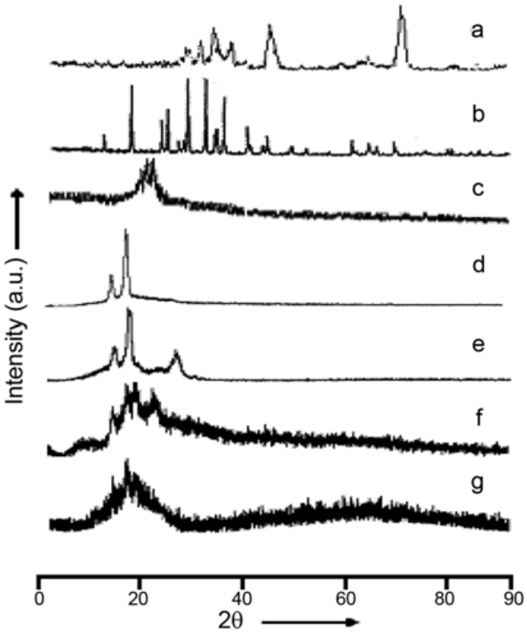

Figure 4. X-ray diffractograms of (a) Al_2O_3 nano particles, (b) pure NH_4SCN, (c) PVA:DMSO nanofibers, (d) PVA:DMSO: NH_4SCN nanofibers, (e) PVA:DMSO:NH_4SCN+2 wt% Al_2O_3 nano filler filled nanofibers, (f) PVA:DMSO:NH_4SCN+4 wt% Al_2O_3 nano filler filled nanofibers, and (g) PVA:DMSO:NH_4SCN+6 wt% Al_2O_3 nano filler filled nanofibers.

DSC Studies

DSC thermogram for PVA:DMSO, PVA:DMSO:NH_4SCN, and 2, 4, and 6 wt% Al_2O_3 nano particles filled PVA composite electrolyte nanofibers are shown in Figure 5. All the DSC profiles show significant improvement in thermal

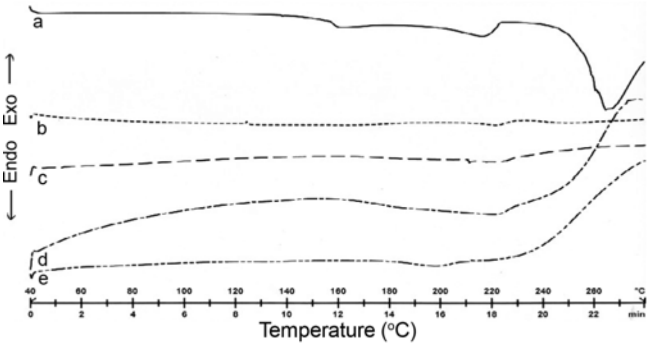

Figure 5. DSC diffractograms of (a) PVA:DMSO nanofibers (──), (b) PVA:DMSO:NH_4SCN nanofibers (·········), (c) PVA:DMSO:NH_4SCN+2 wt% Al_2O_3 nano particles filled nanofibers (— — —), (d) PVA:DMSO:NH_4SCN+4 wt% Al_2O_3 nano particles filled nanofiber (—·—·—·—), and (e) PVA:DMSO:NH_4SCN+6 wt% Al_2O_3 nano particles filled nanofiber (—··—··—··—).

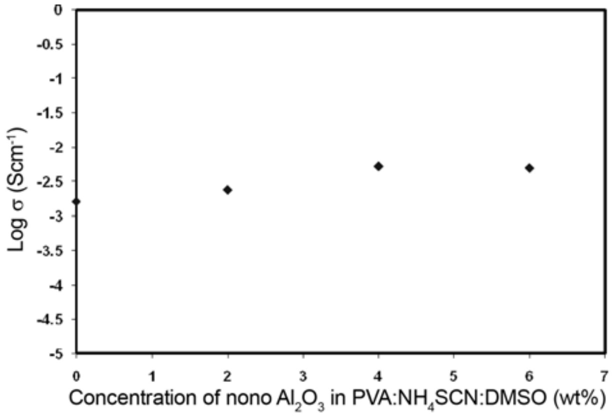

Figure 6. Variation of conductivity of PVA:NH_4SCN:DMSO nanofibers with different concentration of Al_2O_3 nano filler at room temperature.

stability of nanofibers doped with Al_2O_3 nano particles. In thermogram (a) related to PVA:DMSO nanofiber, a peak around 158 ºC is observed. This can be linked to onset temperature of DMSO evaporation trapped within nano fibers in traces. Another peak at 216 ºC is attributed to the melting of crystalline part of PVA. Besides a strong endothermic peak observed at 264 ºC, corresponds to the degradation peak of PVA caused by dehydration of PVA and formation of volatile products [30-34]. Addition of NH_4SCN slightly increased the melting temperature of PVA fibers. This is possibly due to change in chain entanglement/change in chain length of polymer in the presence of high electric field used in preparation of nano fibers. On addition of Al_2O_3, the DSC thermograms didn't reveal any significant change in transition peaks. The insignificant change in enthalpy ($\Delta H \sim 0$) suggests completely amorphous behavior of synthesized electrolyte fiber. It is concluded from these investigations that electrostatic spinning produces an amorphous solid dispersion of NH_4SCN salt and Al_2O_3 nano particles in the PVA matrix resulting in completely amorphous electrolyte nanofibers.

Conductivity Studies

Two probe electrical measurements on PVA:DMSO fibers revealed its conductivity as 2.39×10^{-5} Scm^{-1}, which rose to 1.59×10^{-3} Scm^{-1} upon salt addition in the PVA matrix to form pristine electrolyte. The conductivity value obtained for pristine PVA-NH_4SCN electrolyte fibers is slightly lower than the corresponding result for gel membranes prepared by solution cast technique [3,35,36]. This observation can be associated to significant drying of samples/stretching of chains in the presence of high electric field. In polymer electrolytes the ionic conductivity has been shown to depend upon the number of free charge carriers and improved morphology of the system [3,36]. In the present study, the enhancement in electrical conductivity in pristine PVA-NH_4SCN electrolyte fibers can be ascribed to the porous structure of electrospun membrane and improvement in morphology as witnessed in XRD and DSC studies. This allows greater absorption of NH_4SCN salt within the fiber. Figure 6 depicts variation of ionic conductivity of electrolyte nanofibers as a function of Al_2O_3 concentration. Conductivity behavior shows a gradual increase with filler concentration and it tends to saturate though the change remains within an order of magnitude. This feature is in contrast to conductivity results on gel membranes prepared by solution cast technique where an optimum was achieved for 4 wt% Al_2O_3 content and later it dips. The slight improvement is possibly due to increase in amorphous structure (XRD studies/DSC data). Existence of improved amorphous phase tends to increase conduction pathways for ion transport. Another possibility may be increase in conduction pathways in the presence of nano filler [6,37]. Detailed studies are underway to establish the mechanism of ion transport.

Conclusion

The current preliminary investigation deals with structural, thermal, and electrical characterization of electrospun nanofibers. After doping the PVA fiber with NH_4SCN salt and Al_2O_3 nanoparticles, morphology and ionic conduction in PVA electrospun fibers is seen to improve considerably. Scanning electron microscopy results show fiber diameter to vary in between 1 μm to 500 nm depending up on the flow rate, applied voltage, and filler concentration. XRD profiles of Al_2O_3 nano filled PVA composite electrolyte nanofibers reveal increase in amorphous behaviour upon filler addition. Differential scanning calorimetry measurements show better thermal stability as compared to corresponding gel film. The ionic conductivity of Al_2O_3 nano filled PVA:NH_4SCN electrolyte electrospun fiber reaches 5.31×10^{-3} Scm^{-1} for

4 wt% filler concentration at room temperature which is better than the conductivity of corresponding gel film.

References

1. C. Berthier, W. Gorecki, M. Minier, M. B. Armand, J. M. Chabango, and P. Rigaud, *Solid State Ionics,* **11**, 91 (1983).
2. P. Colomban, "Proton Conductors: Solid, Membrane and Gels-materials and Devices", Cambridge University Press, Cambridge, 1992.
3. A. Awadhia and S. L. Agrawal, *Solid State Ionics*, **178**, 951 (2007).
4. S. Chandra, S. S. Sekhon, and N. Arora, *Ionics*, **6**, 112 (2000).
5. S. K. Patel, R. B. Patel, A. Awadhia, N. Chand, and S. L. Agrawal, *Pramana*, **69**, 467 (2007).
6. J. Adebahr, N. Byrne, M. Forsyth, D. R. MacFarlane, and P. Jacobsson, *Electrochimica Acta*, **48**, 2099 (2003).
7. H. Kataoka, Y. Saita, T. Sakai, E. Quartarone, and P. Mustarelli, *J. Phys. Chem. B*, **104**, 11460 (2000).
8. Y. Saito, H. Kataoka, and A. M. Stephan, *Macromolecules*, **34**, 6955 (2001).
9. K. M. Abraham, *Electrochim. Acta*, **38**, 28 (1993).
10. J. R. Kim, S. W. Choi, S. M. Jo, W. S. Lee, and B. C. Kim, *Electrochim. Acta*, **50**, 69 (2004).
11. A. D. Pasquier, P. C. Warren, D. Culver, A. S. Gozdz, G. G. Amatucci, and J. M. Tarascon, *Solid State Ionics*, **135**, 249 (2000).
12. K. K. Baumgarten, *J. Colloid Interface Sci.*, **36**, 71 (1971).
13. S. Koombhongse, W. Liu, and D. H. Reneker, *J. Polym. Sci., Part B: Polym. Phys.*, **39**, 2598 (2001).
14. C. Burger, B. S. Hsiao, and B. Chu, *Annu. Rev. Mat. Res.*, **36**, 333 (2006).
15. Y. Ding, P. Zhang, Z. Long, Y. Jiang, and F. Xu, *Sci. Technol. Adv. Mater.*, **9**, 4 (2008).
16. S. W. Choi, S. M. Jo, W. S. Lee, and Y. R. Kim, *Adv. Mater.*, **15**, 23 (2003).
17. A. Laforgue, L. Robitaille, A. Mokrini, and A. Ajji, *Macromol. Mater. Eng.*, **292**, 1229 (2007).
18. X. Lu, J. Zhou, Y. Zhao, Y. Qiu, and J. Li, *Chem. Mater.*, **20**, 3420 (2008).
19. P. K. Panda and S. Ramakrishna, *J. Mater. Sci.*, **42**, 2189 (2007).
20. Y. Srivastava, M. Marquez, and T. Thorsen, *J. Appl. Polym. Sci.*, **106**, 3171 (2007).
21. K. Zhang, L. L. Zhang, X. S. Zhao, and J. Wu, *Chem. Mater.*, **22**, 1392 (2010).
22. X. Yang, C. Shao, and Y. Liu, *J. Mater. Sci.*, **42**, 8470 (2007).
23. A. R. Uribe, L. Arizmendi, M. E. R. Guzmán, S. S. Guzmán, and R. C. Silva, *Appl. Mater. Interf.*, **1**, 2502 (2009).
24. L. Longenberger and G. Mills, *J. Phys. Chem.*, **99**, 475 (1995).
25. P. K. Khanna, R. Gokhale, V. V. V. S. Subharao, B. K. Das, and C. V. V. Satyanarayana, *Mater. Chem. Phys*., **92**, 229 (2005).
26. J. Bai, Y. Li, S. Yang, J. Du, S. Wang, J. Zheng, Y. Wang, Q. Yang, X. Chen, and X. Jing, *Solid State Communications*, **141**, 292 (2007).
27. E. H. Sanders, K. A. Mcgrady, G. E. Wnek, C. A. Edmondson, J. M. Mueller, J. J. Fontanella, S. Suarez, and S. G. Greenbaum, *J. Power Sources*, **129**, 55 (2004).
28. S. W. Lee, Y. U. Kim, S. S. Choi, T. Y. Park, Y. L. Joo, and S. G. Lee, *Mater. Lett.*, **61**, 889 (2007).
29. G. Verreck, I. Chun, J. Peeters, J. Rosenblatt, and M. E. Brewster, *Pharmaceutical Research*, **20**, 5 (2003).
30. C. A. Finch, "Polyvinyl Alcohol: Properties & Applications", John Wiley & Sons, Bristol, 1973.
31. K. C. Gong and H. S. Cai in "Solid State Ionics" (G. Nazri, R. A. Huggins, and D. F. Shriver Eds.), Vol. 135, p.377, Pittsburgh: Materials Research Society, 1989.
32. P. N. Gupta and K. P. Singh, *Solid State Ionics*, **86-88**, 319 (1996).
33. P. K. Shukla and S. L. Agrawal, *Bull. Electrochem.*, **12**, 732 (1996).
34. P. K. Shukla and S. L. Agrawal, *J. Pure & Appl. Phy.*, **38**, 53 (2000).
35. S. L. Agrawal and A. Awadhia, *Bull. Mater. Sci.*, **27**, 523 (2004).
36. N. Chand, N. Rai, S. L. Agrawal, and S. K. Patel, *Communicated to Bull. Mater. Sci.,* 2010.
37. N. Chand, S. L. Agrawal, M. Singh, and N. Rai in "Solid State Ionics" (B. V. R. Chowdari, H. Liu, W. Chen, Q. Xu, and Z. Yu Eds.), p.931, Wuhan University of Technology Press, Wuhan, China, 2010.